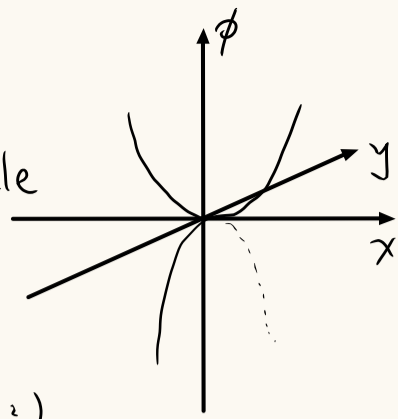


1. Paul trap / Radio-frequency trap

time-varying potential $\phi = \frac{V_0}{2r_0^2} \cos(\omega_{rf} t) (x^2 - y^2) \sim \text{saddle}$
 dynamical trapping



Generally in 3D, $\phi = \underbrace{\frac{V_0}{2r_0^2} (\alpha x^2 + \beta y^2 + \gamma z^2)}_{dc} + \underbrace{\frac{V_{rf}}{2r_0^2} \cos(\omega_{rf} t) (\alpha' x^2 + \beta' y^2 + \gamma' z^2)}_{rf}$

Laplace's equation $\Rightarrow \begin{cases} \alpha + \beta + \gamma = 0 \\ \alpha' + \beta' + \gamma' = 0 \end{cases}$

Choose $\alpha = \beta = \gamma = 0$, and to choose a cylindrically symmetric trap, we need $\alpha' = \beta' = -2\gamma' = 1$
 $\Rightarrow \phi = \frac{V_{rf}}{2r_0^2} \cos(\omega_{rf} t) (x^2 + y^2 - 2z^2) = \frac{V_{rf}}{2r_0^2} \cos(\omega_{rf} t) (r^2 - 2z^2)$
 Cartesian Coordinate Cylindrical Coordinate

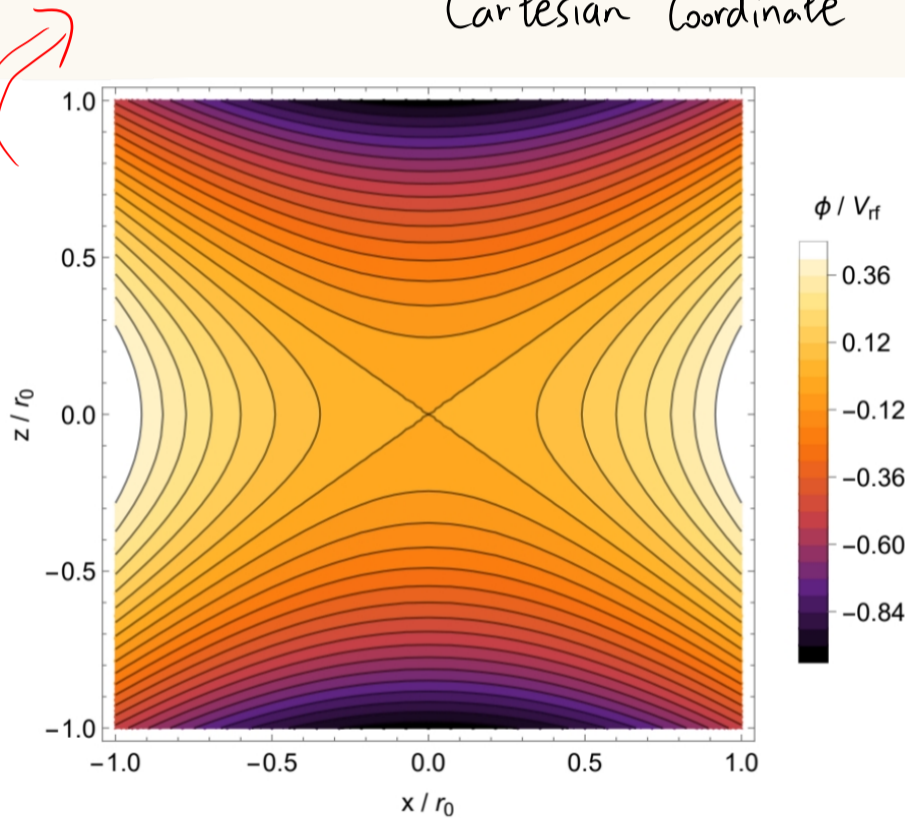
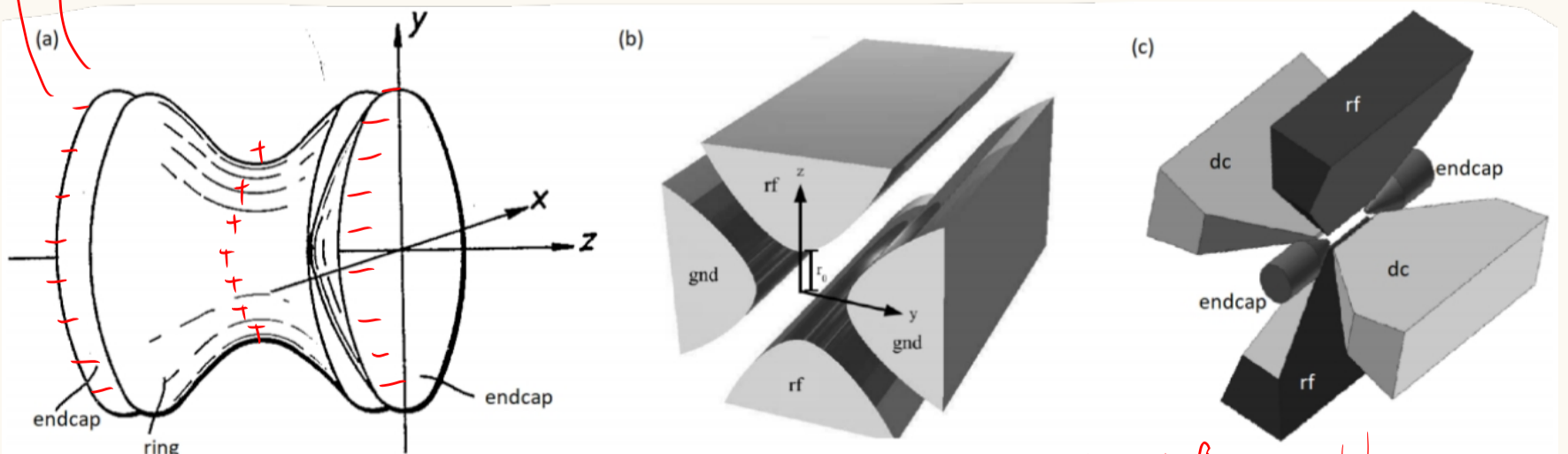


Figure 6.1: Electrostatic potential in the xz -plane for a 3D rf ion trap. The potential has cylindrical symmetry about the z -axis. The values of the contours correspond to Eq. (6.4) at $t = 0$.



$$\begin{cases} \gamma = -\alpha - \beta \\ \alpha' = -\beta', \gamma' = 0 \end{cases}$$

Figure 6.2: Electrode geometries for making rf traps. (a) Cylindrically symmetric 3D rf trap. (b) Linear rf trap with no confinement along the long direction. (c) Linear rf trap with endcap electrodes for static confinement along the long direction.

used for trapping linear strings of ions

Consider an ion of charge e and mass m in a potential of the general form. Consider the x -direction and set $\alpha = \alpha' = 1$, the equation of motion:

$$\frac{d^2 x}{dt^2} = -\frac{e}{mr_0^2} [V_0 + V_{rf} \cos(\omega_{rf} t)] x$$

$$\tau = \frac{\omega_{rf} t}{2}, \quad a_x = \frac{4eV_0}{mr_0^2 \omega_{rf}^2}, \quad q_x = \frac{2eV_{rf}}{mr_0^2 \omega_{rf}^2}$$

$$\frac{d^2 x}{d\tau^2} + [a_x - 2q_x \cos(2\tau)] x = 0 \quad \text{Mathieu equation}$$

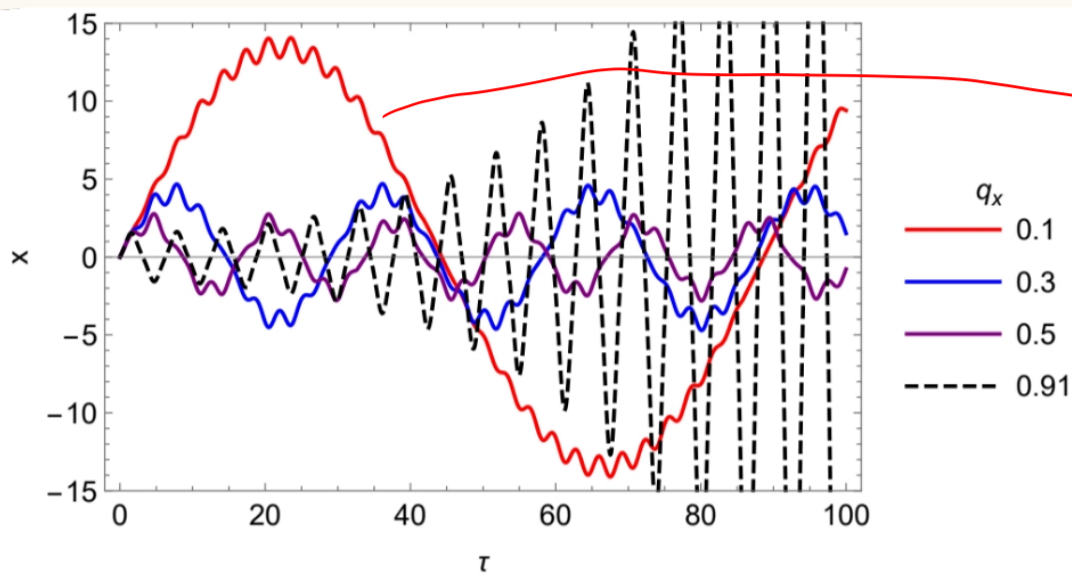


Figure 6.3: Solutions to the Mathieu equation, with $a_x = 0$ and various values of q_x . The motion becomes unstable for $q_x > 0.9$ (black dashed line).

micromotion: a small amplitude oscillation at the rf frequency
 ↕ superimpose
 secular motion: a slower and larger amplitude oscillation

$q_x \nearrow$, the frequencies of the two oscillations approach one another

no dc potential

The behavior at small q_x suggests $x = x_f + x_s$ (fast and slow oscillation), we assume $x_f \ll x_s$, $d^2 x_f / dt^2 \gg d^2 x_s / dt^2$

$$\implies \frac{d^2 x_f}{d\tau^2} = 2q_x \cos(2\tau) x_s$$

Takes x_s to be a constant over the short period of high-frequency oscillation, so that

$$x_f = -\frac{q_x x_s}{2} \cos(2\tau)$$

$$\implies \frac{d^2 (x_s + x_f)}{d\tau^2} = 2q_x \cos(2\tau) (x_s + x_f)$$

$$\frac{d^2 x_s}{d\tau^2} + \frac{d^2 x_f}{d\tau^2} = 2q_x x_s \cos(2\tau) - q_x^2 x_s \cos^2(2\tau)$$

time average over one period of the rf drive

$$\begin{array}{ccc} \downarrow & & \downarrow \\ 0 & & 0 \\ & & \downarrow \\ & & \frac{1}{2} \end{array}$$

$$\implies \frac{d^2 x_s}{d\tau^2} = -\frac{q_x^2}{2} x_s$$

$$\implies \frac{d^2 x_s}{dt^2} = -\left(\frac{e^2 V_{rf}^2}{2m^2 r_0^4 \omega_{rf}^2} \right) x_s$$

slow motion is that of a harmonic oscillator of angular frequency $\omega_x = \frac{eV_{rf}}{\sqrt{2} m r_0^2 \omega_{rf}}$
 $\omega_z = 2\omega_x = 2\omega_y$ for a cylindrical trap

macroscopic ion traps \sim trap frequencies \sim 1 MHz

microscopic ion traps formed on chips \sim trap frequencies \sim 10-100 MHz

2. Penning trap

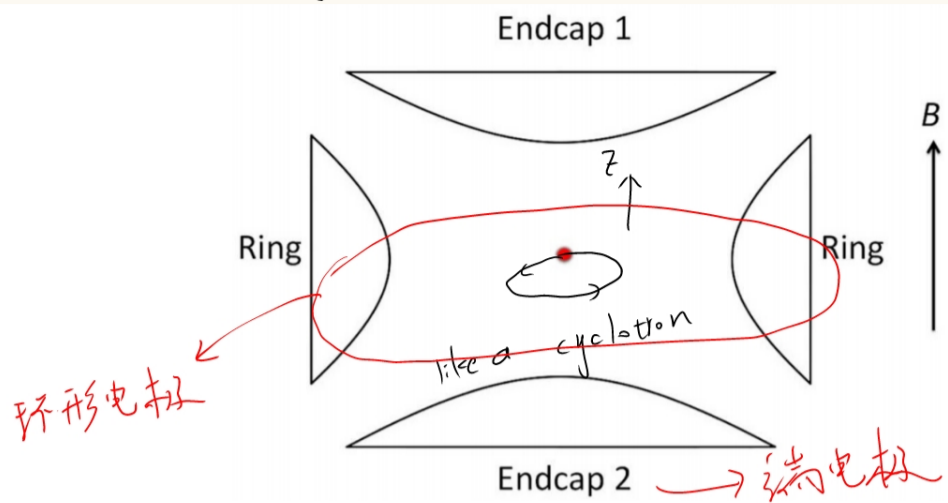
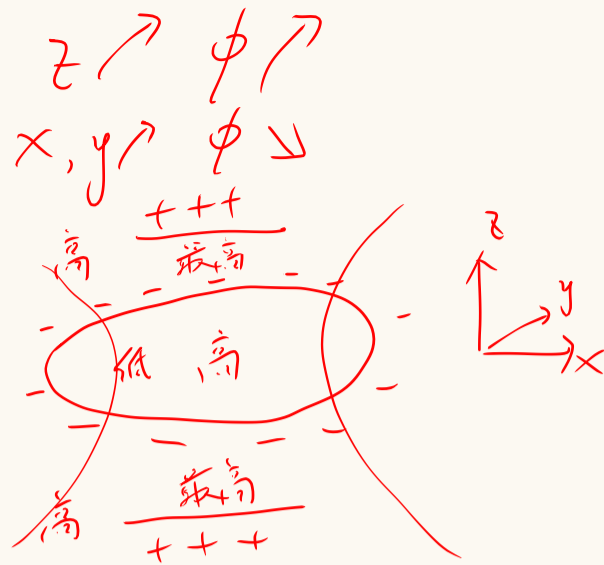


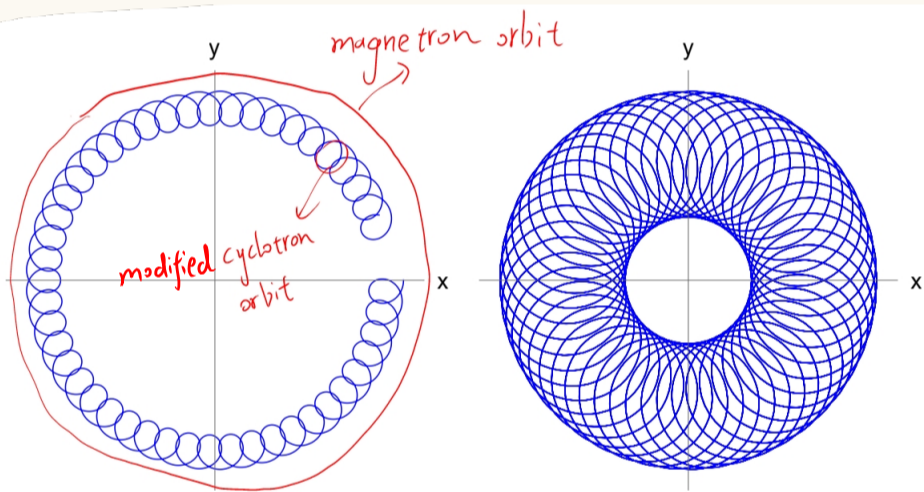
Figure 6.5: Cross section through the electrodes of a Penning trap. The trap has cylindrical symmetry about the vertical axis. The two endcaps are electrically connected and a dc voltage is applied between the ring and the endcaps.



$$\phi = \frac{V_0}{2r_0^2} \left(z^2 - \frac{1}{2}(x^2 + y^2) \right)$$

$$\begin{cases} \vec{E} = -\nabla\phi = -\frac{V_0}{r_0^2} \left(z\vec{e}_z - \frac{1}{2}(x\vec{e}_x + y\vec{e}_y) \right) \\ \vec{B} = B\vec{e}_z \\ \vec{F} = e(\vec{E} + \vec{v} \times \vec{B}) \end{cases} \Rightarrow$$

$$\begin{cases} \dot{x} = \frac{1}{2}\omega_z^2 x + \omega_c y \\ \dot{y} = \frac{1}{2}\omega_z^2 y - \omega_c x \\ \dot{z} = -\omega_z^2 z \end{cases} \quad \begin{array}{l} \text{cyclotron frequency } \omega_c = \frac{eB}{m} \\ \text{axial frequency } \omega_z = \sqrt{\frac{eV_0}{mr_0^2}} \end{array}$$



$$u = x + iy$$

$$\dot{u} = \frac{1}{2}\omega_z^2 u - i\omega_c u$$

$$\Downarrow \text{solution of the form } u = A e^{-i\omega t}$$

$$\omega^2 - \omega_c \omega + \frac{1}{2}\omega_z^2 = 0$$

$$\begin{cases} \omega_+ = \frac{1}{2}(\omega_c + \sqrt{\omega_c^2 - 2\omega_z^2}) & \text{modified cyclotron frequency} \\ \omega_- = \frac{1}{2}(\omega_c - \sqrt{\omega_c^2 - 2\omega_z^2}) & \text{magnetron frequency } \omega_m \end{cases}$$

$$\omega_+ \gg \omega_z \gg \omega_-$$

Figure 6.6: Example trajectories in the radial plane of an ion in a Penning trap. Small circles are cyclotron orbits, the larger one is the magnetron orbit.

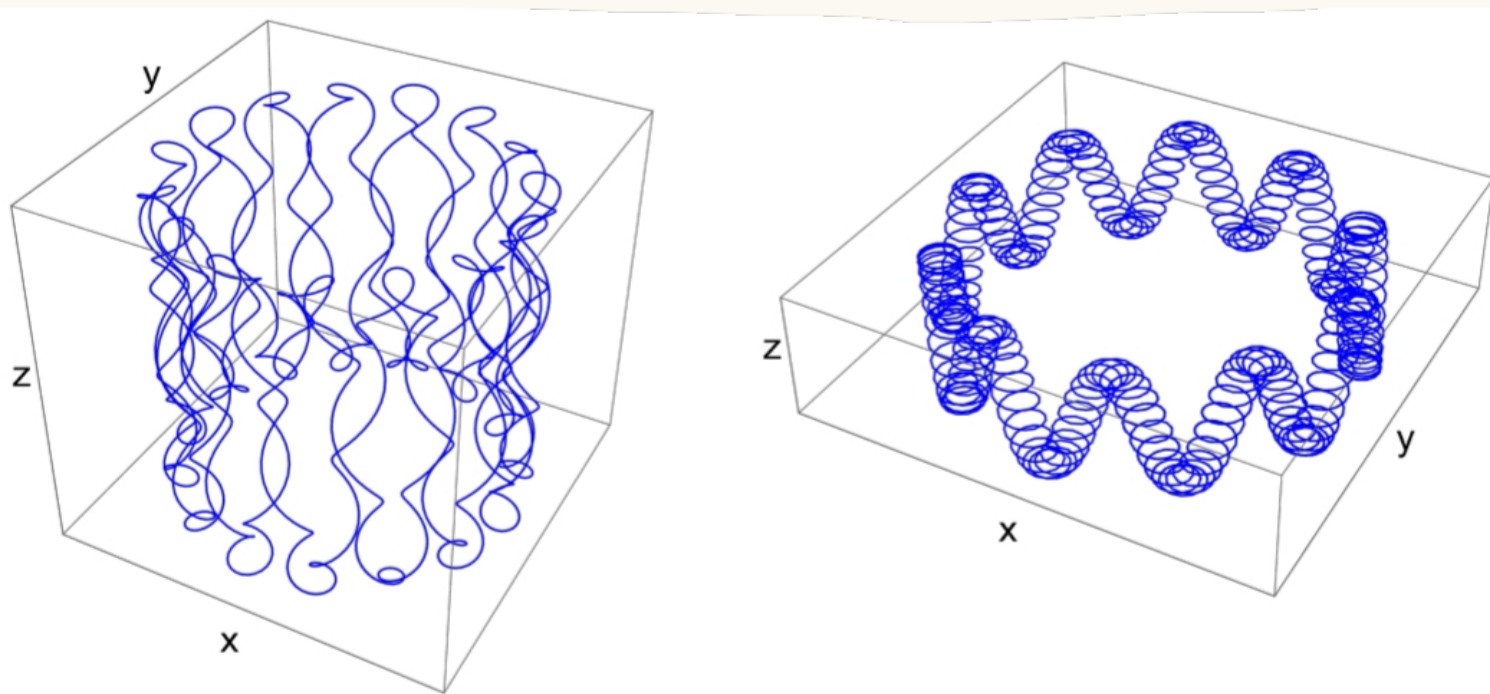


Figure 6.7: Examples of three-dimensional trajectories of an ion in a Penning trap.

3. Sideband cooling

4. Trapped ion quantum computing

- Advantages {
- long trap lifetimes
 - long internal-state coherence times
 - strong ion-ion interactions
 - the existence of cycling transitions that can be used for coding and qubit readout

① Optical qubits: $^2S_{1/2}$ ground state $|1\rangle$ and $^2D_{5/2}$ excited state $|2\rangle$ ($Be^+, Ca^+, Mg^+, Sr^+, Ba^+$)

e.g. $^{40}Ca^+$

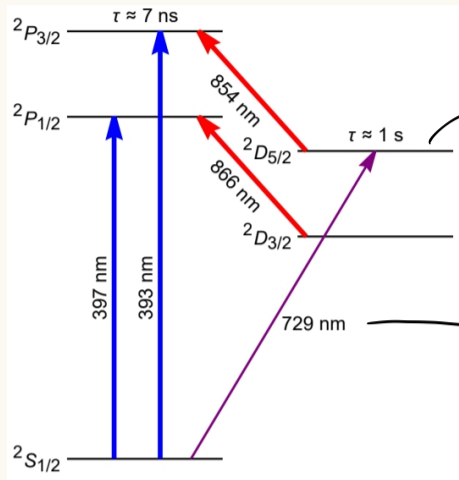


Figure 6.9: Energy levels and transitions of $^{40}Ca^+$.

metastable with a long lifetime

laser pulses at 729 nm used to drive single qubit gate

Readout: turn on the laser cooling light and detect the fluorescence of the ion

- in $|1\rangle \rightarrow$ fluoresces
- in $|2\rangle \rightarrow$ does not ...

② Hyperfine qubits \sim infinite lifetimes

e.g. $^{43}Ca^+$, nuclear spin $I = 7/2$, $F=3$ and $F=4$ hyperfine states

$^2S_{1/2}$, $F = |\frac{1}{2} \pm \frac{7}{2}|$
total angular momentum

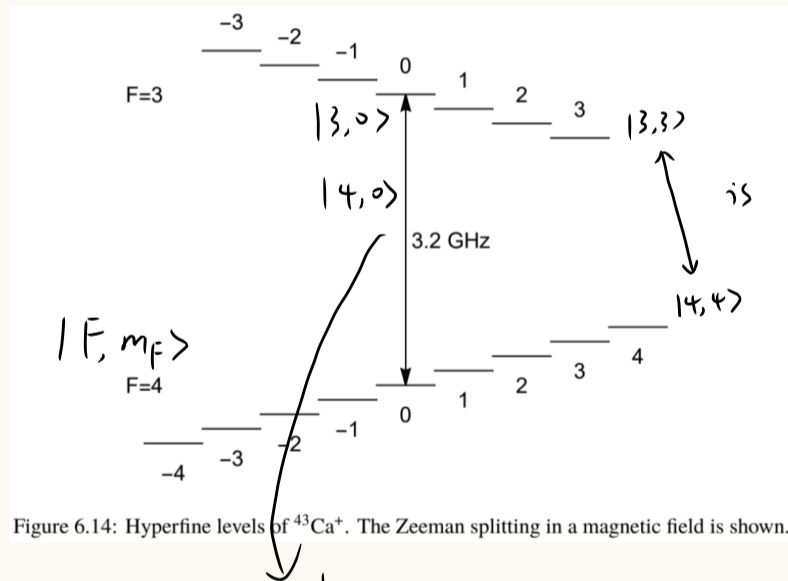
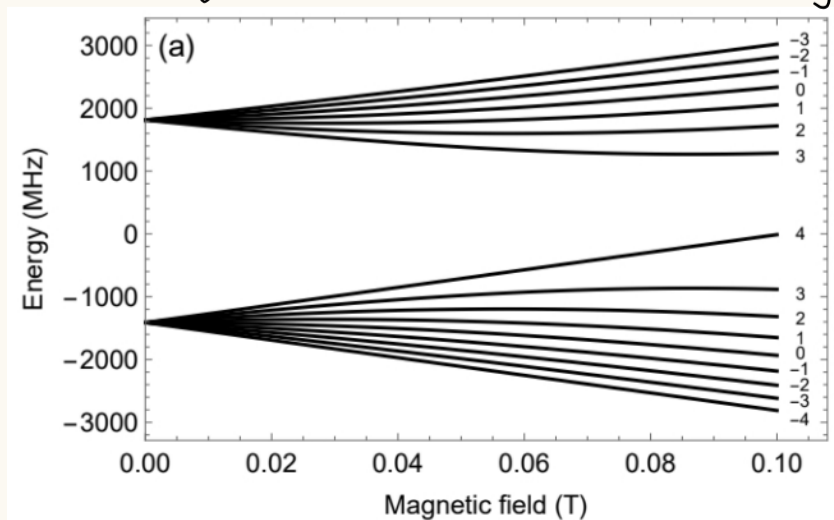


Figure 6.14: Hyperfine levels of $^{43}Ca^+$. The Zeeman splitting in a magnetic field is shown.

is prone to dephasing due to frequency fluctuations caused by magnetic field fluctuations (sensitivity 24.5 GHz/T)

a better choice: have no first-order Zeeman shift at zero field

In practice, a small magnetic field needs to be applied in order to lift the degeneracy, but this qubit still has a small magnetic field sensitivity.



We want to find a different choice of qubit gives zero sensitivity to magnetic field at a particular non-zero field, i.e. $df/dB = 0$ Clock states

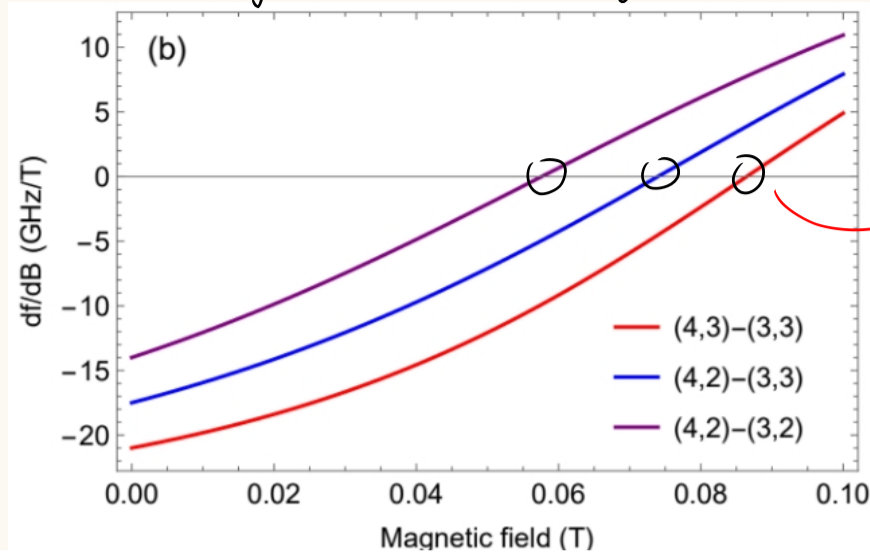
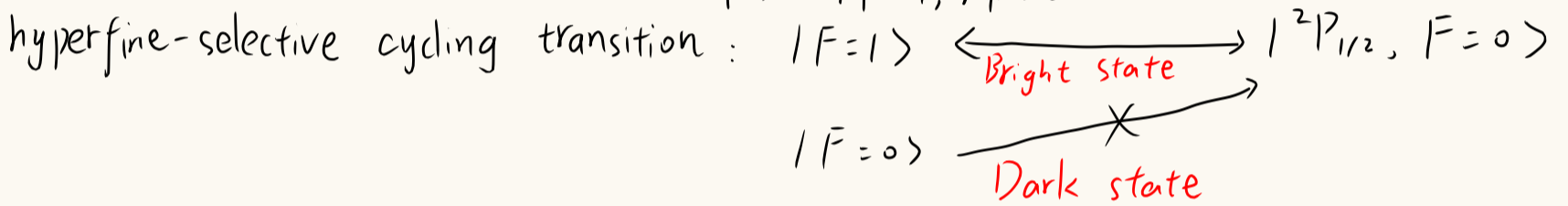


Figure 6.15: (a) Zeeman splitting of the ground state hyperfine components of $^{43}\text{Ca}^+$. (b) Sensitivity of qubit frequency to magnetic field, df/dB , as a function of magnetic field, for a few different qubit choices.

Readout: based on a hyperfine-selective cycling transition.
 e.g. For $^{171}\text{Yb}^+$ $^2S_{1/2} \Rightarrow |0\rangle = |F=0, m_F=0\rangle$
 $|1\rangle = |F=1, m_F=0\rangle$



Here, $|0\rangle = |^2S_{1/2}, F=4\rangle \xrightarrow{\text{shelving}} ^2D_{5/2}$
 $|1\rangle = |^2S_{1/2}, F=3\rangle$

Once the ion reaches $^2D_{5/2}$, it remains there for a long time, because the state has such a long lifetime.
This is called "shelving"

\Downarrow
 cycling transition: $^2S_{1/2} \xleftrightarrow{397\text{nm}} ^2P_{1/2}$
 Bright state: $|1\rangle$
 Dark state: $|0\rangle$ (Because of shelving)

③ Single-qubit gates

The dynamics here are simply that of a two-level atom interacting with light. The light is resonant with the transition. ($\delta = 0$)

light: $\vec{E} = \vec{E}_0 \cos(\omega t + \phi)$

$$\begin{cases} i \frac{dc_1}{dt} = \frac{\Omega}{2} e^{i\phi} c_2 \\ i \frac{dc_2}{dt} = \frac{\Omega}{2} e^{-i\phi} c_1 \end{cases} \Rightarrow \begin{cases} c_1(t) = \cos(\Omega t/2) c_1(0) - i e^{i\phi} \sin(\Omega t/2) c_2(0) \\ c_2(t) = -i e^{-i\phi} \sin(\Omega t/2) c_1(0) + \cos(\Omega t/2) c_2(0) \end{cases}$$

$$c_1(t)|1\rangle + c_2(t)|2\rangle = \begin{pmatrix} c_1(t) \\ c_2(t) \end{pmatrix} = U(t) \begin{pmatrix} c_1(0) \\ c_2(0) \end{pmatrix}, \quad U(t) = \begin{pmatrix} \cos(\Omega t/2) & -i e^{i\phi} \sin(\Omega t/2) \\ -i e^{-i\phi} \sin(\Omega t/2) & \cos(\Omega t/2) \end{pmatrix}$$

When $\phi = 0$

} $\Omega t = \pi/2$ ($\frac{\pi}{2}$ pulse)	$c_1(t) = \frac{1}{\sqrt{2}} (c_1(0) - i c_2(0))$	$\sim 1\rangle \rightarrow \frac{1}{\sqrt{2}} (1\rangle - i 2\rangle)$
	$c_2(t) = \frac{1}{\sqrt{2}} (-i c_1(0) + c_2(0))$	$\sim 2\rangle \rightarrow \frac{1}{\sqrt{2}} (-i 1\rangle + 2\rangle)$
	$\Omega t = \pi$ (π pulse)	$ 1\rangle \rightarrow -i 2\rangle$ $ 2\rangle \rightarrow -i 1\rangle$
$\Omega t = 2\pi$ (2π pulse)	$ 1\rangle \rightarrow - 1\rangle$ $ 2\rangle \rightarrow - 2\rangle$	

For an optical qubit, the transitions are driven using laser pulses.

For a hyperfine qubit (two states have the same parity):

single qubit manipulations { be driven directly in the microwave domain
 (a magnetic dipole transition)
 long wavelength | difficult to address the individual ions ??
 using small microwave transmission lines microfabricated into the chip
 using a Raman transition in the optical domain (a two-photon process)

two lasers: ω_1, ω_2
 $\Delta = \omega_1 - \omega_2 - \omega_{12}$
 $\Delta \gg \Omega_1, \Omega_2, \Gamma$

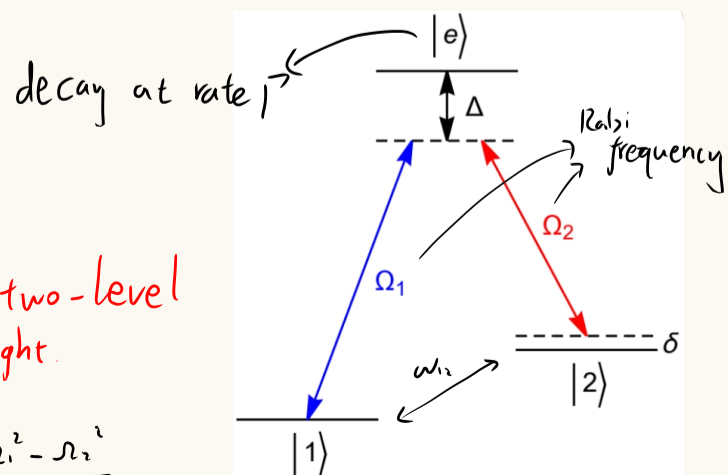


Figure 6.16: Driving a Raman transition

The dynamics are identical to that of a two-level system driven by a single frequency of light.
 effective Rabi frequency $\Omega_{\text{eff}} = \frac{\Omega_1 \Omega_2}{2\Delta}$
 effective two-photon detuning $\delta_{\text{eff}} = \Delta - \frac{\Omega_1^2 - \Omega_2^2}{4\Delta}$

④ Two-qubit gates (fidelities 99.9% ; gate speeds 100 μ s)

normal modes of motion in the axial direction

Centre of Mass (COM) at ω_z oscillate in the same phase and with the same amplitude
 a stretch or breathing motion at $\sqrt{3}\omega_z$ (for two-ion chain) oscillate in opposite directions, the ions closer to centre move less than those near the edges

single ion axial trapping frequency

Choose the breathing mode, assume in the motional ground state

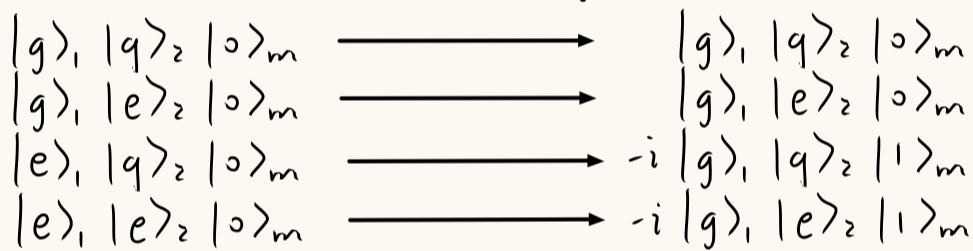
ions: 1, 2

internal states { qubit states $|g\rangle, |e\rangle$
 auxiliary state $|a\rangle$

motional state: $|n\rangle$

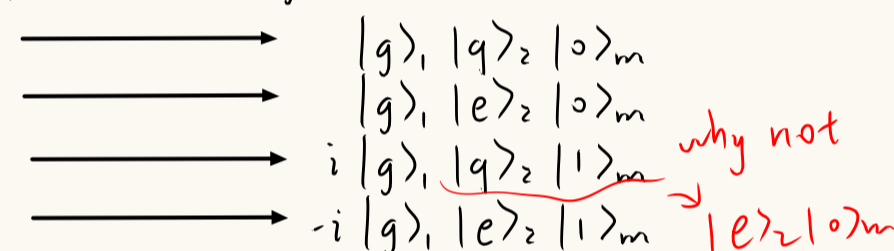
Cirac-Zoller gate (Controlled-Z gate)

π -pulse on the red motional sideband of ion 1



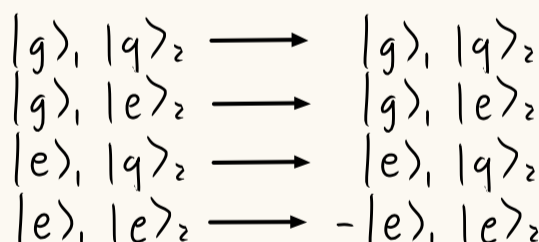
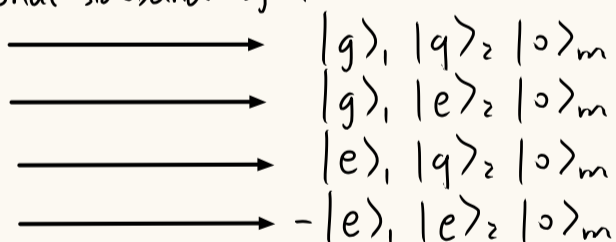
$$\begin{cases} \omega = \omega_0 - \omega t \\ t = \pi / \Omega \end{cases}$$

2π -pulse on the red motional sideband of ion 2



$$\begin{cases} \omega = \omega_0 - \omega t \\ t = 2\pi / \Omega \end{cases}$$

π -pulse on the red motional sideband of ion 1



Drawbacks { ① requires ions to be cooled to the ground state of their collective motion
 ② requires individual addressing of each ion

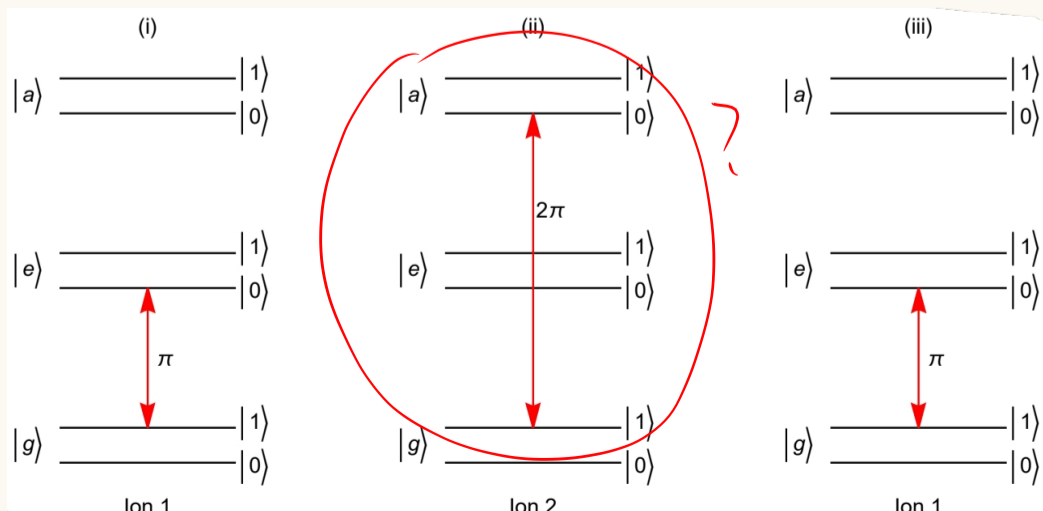


Figure 6.17: Implementation of a controlled-Z gate between a pair of ion qubits. $|g\rangle$ and $|e\rangle$ are the qubit states, and $|a\rangle$ is an auxiliary state. $|0\rangle$ and $|1\rangle$ refer to the (shared) motional state. The steps are applied in sequence. (i) The state of qubit 1 is mapped to the motional state. (ii) A π phase shift is applied to the motional state conditional on the state of qubit 2. (iii) The motional state is mapped back to ion 1.

